

Iterated extended Kalman filter for airborne electromagnetic data inversion

Evgeny Karshakov

To cite this article: Evgeny Karshakov (2019): Iterated extended Kalman filter for airborne electromagnetic data inversion, Exploration Geophysics, DOI: [10.1080/08123985.2019.1593790](https://doi.org/10.1080/08123985.2019.1593790)

To link to this article: <https://doi.org/10.1080/08123985.2019.1593790>



Published online: 28 Apr 2019.



Submit your article to this journal [↗](#)



Article views: 22



View related articles [↗](#)



View Crossmark data [↗](#)



Iterated extended Kalman filter for airborne electromagnetic data inversion

Evgeny Karshakov

V.A. Trapeznikov Institute of Control Sciences of Russian Academy of Sciences (or ICS RAS), Moscow, Russia

ABSTRACT

The iterated extended Kalman filter (IEKF) is a tool within the theory of optimal estimation used for nonlinear problems. The IEKF minimises variance in the estimation error in terms of a probabilistic approach. Despite the special terminology, the Kalman filter algorithm minimises the objective function, representing the normalised squared difference between the measured and calculated vectors for the parameters of a selected model. It works like the weighted least squares method – a conventional method for airborne electromagnetic data inversion. In this article, I describe the essence of the Kalman approach to solving inverse problems. I show how one-dimensional inversion with lateral constraints can be performed in terms of the Kalman filter. The described algorithm takes account of the measurement noise, which is specified as the dispersion of signals in the corresponding measurement channels at high altitude. A specific covariance matrix representation allows use of the corresponding Kalman filter calculation methods. They provide numerical stability of the algorithm. The Kalman approach makes it possible to combine modern techniques used in airborne survey data processing. Some examples of Kalman filter use in frequency-domain airborne data processing are given.

ARTICLE HISTORY

Received 22 August 2018
Accepted 3 March 2019

KEYWORDS

Inversion; Kalman filter; airborne electromagnetics; frequency domain; time domain

Introduction

The Kalman filter (KF) is a widely used tool in optimal state estimation theory (Simon 2006). Although initially formulated for linear problems (Kalman 1960), the algorithm was later extended and applied to nonlinear problems as well. Most KF applications are for problems related to various dynamic systems, but some quite complicated KF algorithms are applied to ill-posed problems (Keppenne and Rienecker 2003).

Conventional methods for airborne electromagnetics (AEM) data processing are apparent resistivity calculation and one-dimensional (1D) inversion, because they provide quick representation of the physical properties of an environment without the need for additional information. Apparent resistivity is calculated as the resistivity of an equivalent homogeneous half-space for each channel in a frequency domain (FD) or time domain (TD). Generally, the geometry of the AEM system, including its altitude, is used in the calculations. 1D inversion calculates parameters for a horizontally layered model in such a way that the modelled response corresponds to the measurements of the AEM system; the geometry is also taken into account. For both methods, it is necessary to solve problems that are ill-posed according to Hadamard (1932). Thus, regularisation is required to provide a unique and stable solution.

According to Chang-Chun et al. (2015), a generally accepted set of 1D inversion methods exists in AEM. Three basic methods are given in Guillemoteau, Sailhac,

and Béhaegel (2011): vertically constrained inversion (VCI), laterally constrained inversion (LCI) and singular value decomposition (SVD). The LCI method described in Guillemoteau, Sailhac, and Béhaegel (2011) uses a reference model provided by previous soundings. All these methods use different techniques to eliminate measurement noise, but the basis of all is minimisation of the following quadratic function:

$$Q = \sum_{j=1}^N [F_j^{obs} - F_j^{cal}(\mathbf{m})]^2, \quad (1)$$

where N is the number of channels in the AEM system, which are used in the processing; F^{obs} is the measurement results and F^{cal} is the solution to the forward problem for the model, with parameters given by vector $\mathbf{m} = (\rho_1, h_1, \rho_2, h_2, \dots)$, where ρ_k is the resistivity and h_k is the thickness of the corresponding layer.

According to Legault (2015), the vast majority of modern AEM systems use the vertical magnetic dipole to transmit the field and the vertical component of the response to interpret. Following a trend for the given frequency ω , I calculate function F in Equation (1) as the vertical component of the response (Zhdanov 2009):

$$H_z(\omega) = -\frac{1}{2\pi} \int_0^\infty u(n_0, z, h_T, \omega) J_0(n_0 r) n_0^2 dn_0, \quad (2)$$

where J_0 is the zero-order Bessel function of the first kind, r is the horizontal shift of the receiver with respect

to the dipole axis, h_T is the altitude of the dipole above the ground, z is the altitude of the receiver and u is two-dimensional (2D) spectrum of the potential of the secondary field:

$$u(n_0, z, h_T, \omega) = \frac{M \cdot \exp(-n_0(z + h))}{2} \cdot \frac{n_1 - n_0 R^*}{n_1 + n_0 R^*}, \quad (3)$$

where M is the amplitude of the dipole moment and R^* is the reduced spectral impedance of the medium. For K layers (the thickness of the bottom layer is considered infinite), the reduced spectral impedance is given as

$$R^* = \tanh \left\{ n_1 h_1 + \tanh^{-1} \left[\frac{n_1}{n_2} \tanh \left(n_2 h_2 + \dots \left(n_{K-1} h_{K-1} + \tanh^{-1} \frac{n_{K-1}}{n_K} \right) \dots \right) \right] \right\},$$

$$n_k = \sqrt{n_0^2 - \frac{i\omega\mu_0}{\rho_k}}, \quad \text{Re } n_k > 0, \quad (4)$$

$\mu_0 = 4\pi \cdot 10^{-7}$ H/m is the magnetic constant, i is the imaginary unit, $\text{Re } n_k$ is the real part of the complex number n_k .

Equations (2)–(4) are sufficient to solve the forward problem in the 1D case and to obtain the function F for AEM FD systems. The real part of Equation (2) gives the in-phase component and the imaginary part gives the quadrature component of the secondary field.

To obtain a model of the TD response, it is enough to convolve the frequency response of the layered model $SH_z(\omega)$ with the known spectrum of the primary field $ST(\omega)$. The components of the frequency response are calculated by using $M = 1$ in Equation (3). Taking into account that the waveform of all AEM TD systems is periodical and symmetrical, and that the receiver frequency response $SR(\omega)$ is bound by the Nyquist frequency at least, it is sufficient to calculate the response for a finite number of odd harmonics of the base frequency (Volkovitsky and Karshakov 2013):

$$H_z(t) = \frac{1}{2\pi} \text{Re} \sum_{k=0}^L SH_z(\omega_k) \cdot ST(\omega_k) \cdot SR(\omega_k) \cdot \exp(-i\omega_k t), \quad \omega_k = (2k + 1)\omega_0, \quad (5)$$

where ω_0 is the base frequency of the primary field, i.e. the minimal frequency in the waveform spectrum; ω_L is the maximum frequency, that can be registered by the receiver, $SR(\omega_k) = 0$ for $k > L$.

Obviously, setting the number of layers $K = 1$ in Equation (4) leads to the forward problem solution for apparent resistivity. According to Fraser (1987), several approaches are used to calculate apparent resistivity as a function of two parameters of FD data.

- (1) In-phase and quadrature part (IQ): ineffective for high resistivity – there is no in-phase response, and for low resistivity – there is an ambiguous quadrature response, not sensitive to resistivity changes.
- (2) Amplitude and flight altitude (AA): most appropriate method, but gives greater noise for high resistivity with respect to method 4, and greater noise for low resistivity with respect to method 3.
- (3) In-phase part and flight altitude (IA): ineffective for high resistivity – there is no in-phase response.
- (4) Quadrature part and flight altitude (QA): ineffective for low resistivity – there is an ambiguous quadrature response.
- (5) Phase and flight altitude (PA): ineffective for high resistivity – phase is not sensitive to resistivity changes.

Each of these methods provides the use of a 2D nomogram for calculating apparent resistivity, which, with the use of modern software packages, enables the desired values to be obtained quickly. Each of these approaches has its advantages and disadvantages, but it is worth noting the following. First, all give different values for resistivity when the real medium differs from a homogeneous half-space, which makes it difficult to switch from one method to another. But we must switch if we want to get the best result for the whole range of resistivity. For example, it is better to switch from AA to QA in case of high resistivity to decrease the noise level. Second, the secondary field for a layered medium differs from the response for a half-space. This leads to poor adequacy of real measurements and calculated in-phase and quadrature parts: the measured quadrature part can be reasonably greater than calculated one for any half-space.

In this article, I suggest using the KF for the following two tasks: first, to combine modern techniques used in 1D inversion; and second, to get a general algorithm for apparent resistivity calculation. The remainder of the article is organised as follows. First, the inverse problem is formulated as a stochastic estimation problem, and it is necessary to apply the KF. For the solution to this problem, I give the equations of the iterated extended KF (IEKF) (Havlik and Straka 2015). The peculiarity of the proposed approach lies in the way of calculating the covariance matrix, an alternative to the methods described by Havlik and Straka (2015). Emphasis is placed on the composition of the estimation-error covariance matrix. How this algorithm implements known approaches is shown: VCI, LCI and SVD. As an example, the described algorithm is applied to data from an AEM FD system, EM4H (Vovenko et al. 2013), for apparent resistivity calculation and for 1D inversion. The last part of the article formulates the conclusions.

Geophysical inversion as a stochastic estimation problem

At each moment j , the measurements of a geophysical system can be represented as a N -dimensional vector \mathbf{z}_j . Assume that the model of the medium at that point is described by a K -dimensional vector of parameters \mathbf{x}_j and the parameters of the field are derived from solution of the forward problem as an N -dimensional vector function $\mathbf{h}_j(\mathbf{x}_j)$:

$$\mathbf{z}_j = \mathbf{h}_j(\mathbf{x}_j) + \mathbf{r}_j, \quad E[\mathbf{r}_j] = 0, \quad E[\mathbf{r}_j \mathbf{r}_j^T] = \mathbf{R}_j \delta_{jk}, \quad (6)$$

where \mathbf{r}_j is a vector of measurement noise, which is modelled as a Gaussian white noise with zero mean and covariance matrix \mathbf{R}_j , $E[\cdot]$ denotes the mean value and δ_{jk} is the Kronecker delta: $\delta_{jk} = 1$ for $j = k$ and $\delta_{jk} = 0$ otherwise.

Also, it is possible to use the time dependence model of the vector \mathbf{x}_j :

$$\mathbf{x}_{j+1} = \mathbf{f}_j(\mathbf{x}_j) + \mathbf{q}_j, \quad E[\mathbf{q}_j] = 0, \quad E[\mathbf{q}_j \mathbf{q}_j^T] = \mathbf{Q}_j \delta_{jk}, \quad (7)$$

where \mathbf{q}_j is a vector of random component that is modelled as Gaussian white noise with zero mean and covariance matrix \mathbf{Q}_j . In essence this matrix represents correlation of medium parameters in neighbouring points. Note, Equation (7) can be considered as a spatial dependence of \mathbf{x} , i.e. matrix \mathbf{Q} and vector \mathbf{f} can be functions of a coordinate along the survey profile (Karshakov and Kharichkin 2008).

The estimation problem is formulated as follows. Assume that the state vector \mathbf{x} satisfies Equation (7). From the measurements \mathbf{z}_j , which satisfy Equation (6), at moments j it is necessary to find vectors $\tilde{\mathbf{x}}_j$ that have minimum deviation from the actual values of \mathbf{x}_j at these points.

Initial estimate $\tilde{\mathbf{x}}_0^-$ of vector of parameters is needed to solve the problem. This estimate does not take any measurements into account and reflects only *a priori* information about the medium. For this vector, a covariance matrix of the *a priori* estimate error is used:

$$\tilde{\mathbf{x}}_0^- = E[\tilde{\mathbf{x}}_0^-], \quad \mathbf{P}_0^- = E[(\mathbf{x}_0 - \tilde{\mathbf{x}}_0^-)(\mathbf{x}_0 - \tilde{\mathbf{x}}_0^-)^T]. \quad (8)$$

This statement of the estimation problem allows us to use the IEKF.

The algorithm of iterated extended Kalman filter

The solution to the estimation problem is given by a sequence of cycles. Each consists of two steps: correction and prognosis. The prognosis step is a transition from *a posteriori* estimates, marked by "+", in point $j-1$, to *a priori* estimates, marked by "-", in point j :

$$\tilde{\mathbf{x}}_j^- = \mathbf{f}_{j-1}(\tilde{\mathbf{x}}_{j-1}^+),$$

$$\mathbf{P}_j^- = \mathbf{A}_{j-1} \mathbf{P}_{j-1}^+ \mathbf{A}_{j-1}^T + \mathbf{Q}_{j-1}, \quad \mathbf{A}_{j-1} = \frac{\partial \mathbf{f}_{j-1}}{\partial \mathbf{x}}. \quad (9)$$

There are several effective methods for severely nonlinear models (Equation 7). They take into account the nonlinearity of \mathbf{f} in different ways, i.e. sigma-point algorithm, unscented filter, etc. (Simon 2006). However, the deterministic part \mathbf{f} in Equation (7) is usually unknown because our knowledge about the medium is minimal. All the uncertainty is put into the random part \mathbf{q} . So, in most cases, the following simple model can be used in Equation (9): $\mathbf{f}(\mathbf{x}) = \mathbf{x}$, $\mathbf{A} = \mathbf{I}$.

The correction step is a transition from an *a priori* estimate to an *a posteriori* estimate at moment j :

$$\begin{aligned} \tilde{\mathbf{x}}_j^{k+} &= \tilde{\mathbf{x}}_j^{k-} + \mathbf{K}_j^k (\mathbf{z}_j - \mathbf{h}_j(\tilde{\mathbf{x}}_j^{k-})), \quad \mathbf{P}_j^{k+} = (\mathbf{I} - \mathbf{K}_j^k \mathbf{H}_j^k) \mathbf{P}_j^{k-}, \\ \mathbf{K}_j^k &= \mathbf{P}_j^{k-} \mathbf{H}_j^{kT} [\mathbf{H}_j^k \mathbf{P}_j^{k-} \mathbf{H}_j^{kT} + \mathbf{R}_j]^{-1}, \quad \mathbf{H}_j^k = \frac{\partial \mathbf{h}_j(\tilde{\mathbf{x}}_j^{k-})}{\partial \mathbf{x}}. \end{aligned} \quad (10)$$

Function $\mathbf{h}(\mathbf{x})$ in Equation (10) is severely nonlinear, see Equations (2) and (5). That is why several iterations are needed during the correction step. The upper index k in Equation (10) designates the iteration number. During each step, the Jacobian matrix \mathbf{H} and filter coefficient \mathbf{K} should be recalculated. The breaking condition for the iteration procedure is met when the following value reaches its minimum:

$$\|\mathbf{z}_j - \mathbf{h}_j(\tilde{\mathbf{x}}_j^{k+})\| = \sqrt{(\mathbf{z}_j - \mathbf{h}_j(\tilde{\mathbf{x}}_j^{k+}))^T \mathbf{R}^{-1} (\mathbf{z}_j - \mathbf{h}_j(\tilde{\mathbf{x}}_j^{k+}))}. \quad (11)$$

If the measurement noise is Gaussian, the minimum of Equation (11) corresponds to the maximum likelihood estimation – maximum of the corresponding distribution function (Simon 2006).

During each iteration step, the following operations should be made:

$$\tilde{\mathbf{x}}_j^{k-} = \tilde{\mathbf{x}}_j^{k-1+}, \quad \mathbf{P}_j^{k-} = \frac{\|\mathbf{z}_j - \mathbf{h}_j(\tilde{\mathbf{x}}_j^{k-1+})\|^2}{\|\mathbf{z}_j - \mathbf{h}_j(\tilde{\mathbf{x}}_j^{k-1-})\|^2} \mathbf{P}_j^{k-1-}. \quad (12)$$

This empirical formula for recalculation of the covariance matrix \mathbf{P} , not common for the IEKF, avoids too rapid a reduction of its norm, because nonlinearity is not taken into account in Equation (10) for \mathbf{P} .

One-dimensional inversion

All the formalism presented above can be applied to various inversion problems that are not necessarily related to AEM. Further, I consider the details of 1D inversion in case of an AEM survey.

First, let us remember that the resistivity of rock follows a log normal distribution (Palacky 1987), so I consider \mathbf{x} as a logarithm of \mathbf{m} from Equation (1).

In the case of the AEM survey, matrix \mathbf{R} can be obtained from calibration flight data. Such flights are performed at high altitude, as a rule 500–700 m above the ground, so the secondary field is negligible

(Vovenko et al. 2013). The statistical characteristic of the signals describes matrix \mathbf{R} completely. The simplest way is to set it as a diagonal matrix in which the diagonal elements are the signal dispersions for the corresponding channel.

As a matter of fact, matrix \mathbf{Q} describes the possible limits of the variation in model parameters from one measurement point to another: its diagonal elements are the dispersions of increment/decrement of the corresponding parameters. Greater variability of the model is required for a greater distance between measurement points. Thus, it is reasonable to set the variability per metre using matrix \mathbf{Q}^1 and calculate matrix \mathbf{Q}_j as $\mathbf{Q}_j = v_j^2 \mathbf{Q}^1$, where v_j is the current velocity of the carrier of the AEM system. In this case, the model itself may be trivial $\mathbf{f}_j(\mathbf{x}_j) = \mathbf{x}_j$.

Finally, matrix \mathbf{P}_0^- , which characterises the adequacy of *a priori* information about the model, should contain the dispersions of the errors for the corresponding parameters in the main diagonal and their correlation coefficients outside it.

When discussing the methods of 1D inversion, it should be noted that Equation (10) is equivalent to the traditional forms for SVD, VCI and LCI (Jupp and Vozoff 1975; Guillemoteau, Sailhac, and Béhaegel 2011). The equivalence follows from the matrix inversion lemma (Simon 2006). It is important to mention that in case of VCI and LCI, the thickness of each layer is fixed.

According to Guillemoteau, Sailhac, and Béhaegel (2011), the VCI method suggests using a matrix with non-diagonal elements as a stabiliser. In terms of the KF, it is equivalent to setting non-diagonal elements in matrix \mathbf{P}^- , which are correlations of the resistivity of layers. The LCI method suggests using a diagonal matrix as a stabiliser. In terms of the KF, it is equivalent to using the prognosis step, where matrix \mathbf{Q}^1 represents the variability in resistivity per metre, as mentioned above. In case of the LCI, it is reasonable to apply the Kalman smoothing algorithm (Simon 2006). The main idea is to apply one KF from the beginning to the end of the profile being processed, another KF from the end to the beginning, and then to combine forward and backward estimates according to their covariance matrixes.

For numerical stability of KF, matrix \mathbf{P} is usually represented by its Cholesky or LDL decomposition: $\mathbf{P} = \mathbf{S}\mathbf{S}^T$ or $\mathbf{P} = \mathbf{L}\mathbf{D}\mathbf{L}^T$, where \mathbf{S} is lower triangular matrix or square root of \mathbf{P} , \mathbf{L} is lower unit triangular matrix and \mathbf{D} is diagonal matrix. Simon (2006) describes the KF algorithm for these forms of \mathbf{P} . He also describes methods of reducing the order of the filter, which is equivalent to the SVD method.

Note, we can evaluate the estimation quality if we have the estimation error covariances. For example, we can use the so-called stochastic estimability measure (Golovan and Parusnikov 1998), which can be calculated

as follows:

$$\mu_j(\mathbf{c}) = 1 - \sqrt{\frac{\mathbf{c}^T \mathbf{P}_j^+ \mathbf{c}}{\mathbf{c}^T \mathbf{P}_j^- \mathbf{c}}}, \quad (13)$$

where vector \mathbf{c} defines the value of interest, e.g. $\mathbf{c} = (1, 0, \dots, 0)^T$ gives the estimability measure of \mathbf{x}_{j1} , and $\mathbf{c} = (0, 1, 1, 0, \dots, 0)^T$ shows the estimation quality of $\mathbf{x}_{j2} + \mathbf{x}_{j3}$. Roughly speaking, the stochastic estimability measure shows how the current set of measurements improves estimation of the parameter $\mathbf{c}^T \mathbf{x}$. From Equation (13) it follows that the better estimation, the closer μ_j is to 1, and small values of μ_j mean poor observability of the parameter related to \mathbf{c} .

Frequency domain data processing

To illustrate this method, I consider calculation of the apparent resistivity, or resistivity of equivalent homogeneous half-space, and 1D inversion for FD AEM data of the system EM4H (Vovenko et al. 2013). Its application to TD data inversion is presented by Karshakov and Moilanen (2018). EM4H has a vertical magnetic dipole fixed to the fuselage of an aircraft and a three-component receiver towed by a flexible 70-m cable. The system transmits an alternating magnetic field at four frequencies (130, 520, 2080 and 8330 Hz) and measures the in-phase and quadrature components of the response (Figure 1). The altitude of the aircraft is controlled by a radar altimeter. In addition, the system measures the position of the receiver with respect to the transmitter. As a result, the sum of receiver and transmitter altitudes ($z + h$) and the horizontal shift of the receiver are obtained, which are required in Equation (3) to calculate the secondary field (Equation 2).

It is necessary to calculate the resistivity of the equivalent homogeneous half-space for each frequency at each point where in-phase (real) and quadrature (imaginary) components of the response are measured. I suggest applying IEKF with in-phase and quadrature components in each frequency as measurements, the sum of receiver and transmitter altitudes ($z + h$), and the horizontal shift of receiver r as parameters in the forward problem solution. In this case, the dimension of the vector of parameters \mathbf{x} is 1 and it contains the logarithm of apparent resistivity only. The vector of measurements \mathbf{z} has dimension 2 and contains the in-phase and quadrature components of the response.

Figure 2 shows the result of IEKF in comparison with resistivity calculated using the nomogram method on the base of quadrature response and flight altitude (QA-nomogram). It is clear that the inversion with the IEKF provides solution uniqueness and efficiency for different resistivity values. For the nomogram method, there are serious difficulties at frequencies of 2 and 8 kHz. The quadrature component of the response is close to the maximum value and has an ambiguity and weak dependence on resistivity.

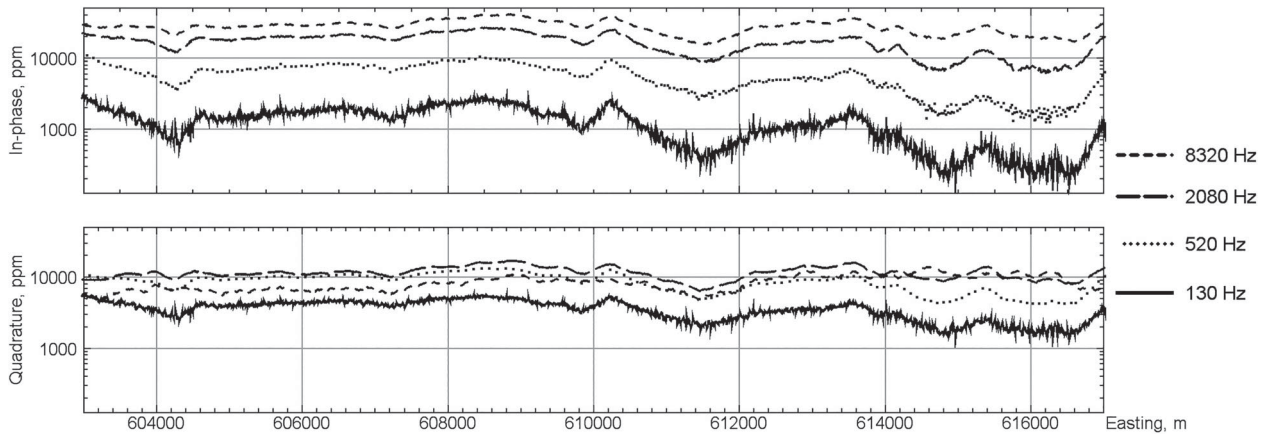


Figure 1. In-phase (upper) and quadrature (lower) measurements at four frequencies of the EM4H system.

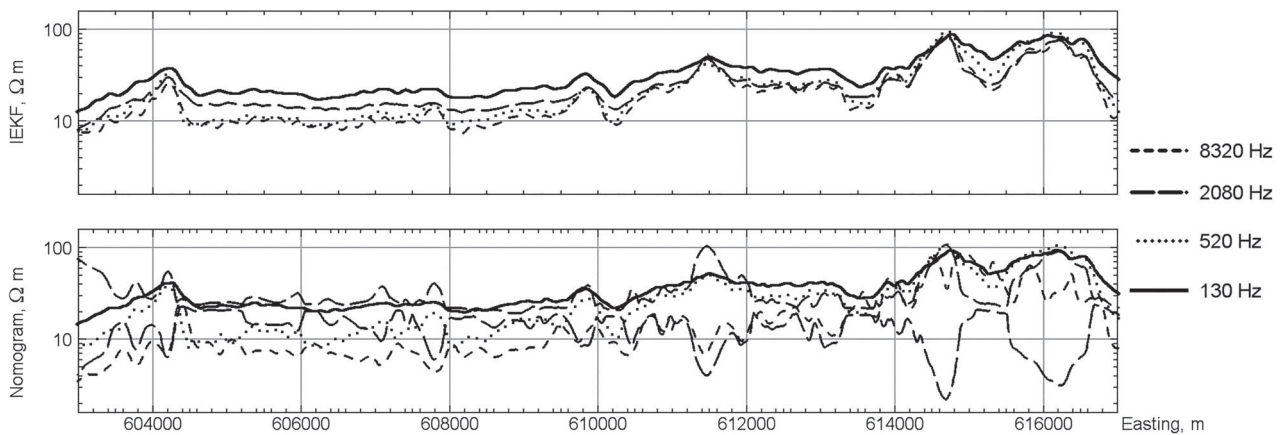


Figure 2. Apparent resistivity obtained using the IEKF (upper) and QA-nomogram (lower) methods. Two nomogram solutions are presented for 2 kHz, a hard choice between the conductive and resistive variants.

Of course, this half-space inversion experiment is not enough. I use different information for the IEKF approach and the “nomogram” approach. As already mentioned, the AA algorithm is the most appropriate. But there is a disadvantage: the amplitude always includes the noise of both the in-phase and quadrature components. The IEKF will reduce the weight of the corresponding component, if it is not sensitive to the resistivity changes. Unfortunately, this is much harder to illustrate. The point of Figure 2 was to show the IEKF solution uniqueness and efficiency for different resistivity values.

For the same data set (Figure 1), I present the results of 1D inversion. First, I present an SVD-like approach. Let us consider the model of homogeneous half-space, so the vector of parameters \mathbf{x} contains the logarithm of resistivity only, whereas the vector of measurements \mathbf{z} has dimension 8 and contains the in-phase and quadrature components of the response at the four frequencies. Figure 3 shows the inversion result together with residuals (Equation 11) and the estimability measure (Equation 13). Despite good estimability, the residuals are > 3 in more than 50% of the points. Statistically,

this means that the model does not fit the measurements. So, it is reasonable to consider a two-layered model.

Figure 4 shows the inversion results for three-dimensional (3D) state vector \mathbf{x} (resistivity logarithm of two layers and the upper layer thickness logarithm). The half-space from the previous step was used as an initial estimate. The residuals now show that the model fits perfectly – they are ~ 1 . At the same time, estimability measures of all three estimated parameters are quite sensitive to changes in the resistivity model. In particular, the measures decrease significantly at points that tend to a half-space model. For example, at points with easting coordinate 604250, 609850, 611450 and 616500, we can see local minima of estimability measures, and at the same points the residual for the half-space model is close to 1 (Figure 3); even the apparent resistivities are close to each other (Figure 2). This makes it hard to detect a resistivity boundary at these points.

Although the measurement vector dimension is much greater than the dimension of parameters vector: $\dim \mathbf{z} = 8$, $\dim \mathbf{x} = 3$, we can conclude, that a three-layered model will be overcomplicated. Moreover, the

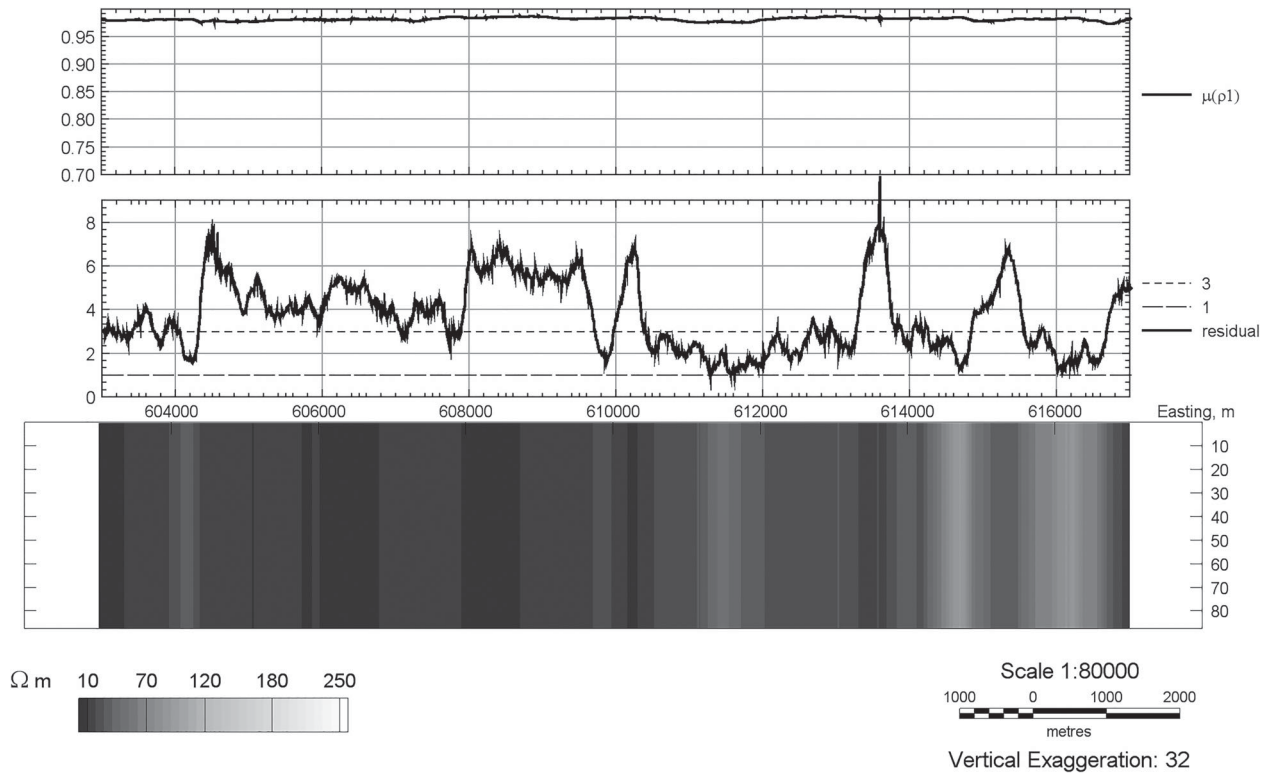


Figure 3. SVD-like 1D inversion for the half-space model (bottom), residuals (centre) and stochastic estimability measure (lower). ρ_1 , resistivity of the half-space.

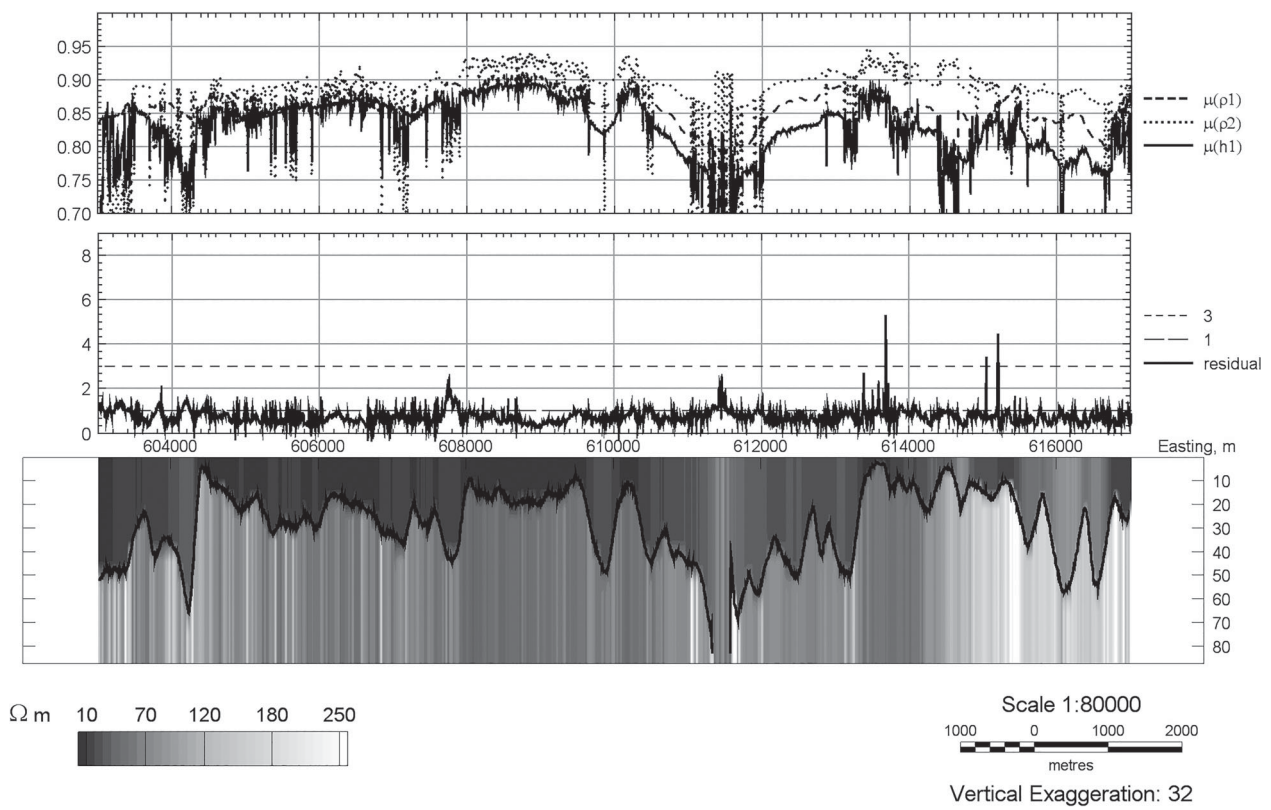


Figure 4. SVD-like 1D inversion for the two-layered model (bottom), residuals (centre) and stochastic estimability measures for three parameters (lower). ρ_1 , resistivity of the upper layer; ρ_2 , resistivity of the bottom layer; h_1 , thickness of the upper layer.

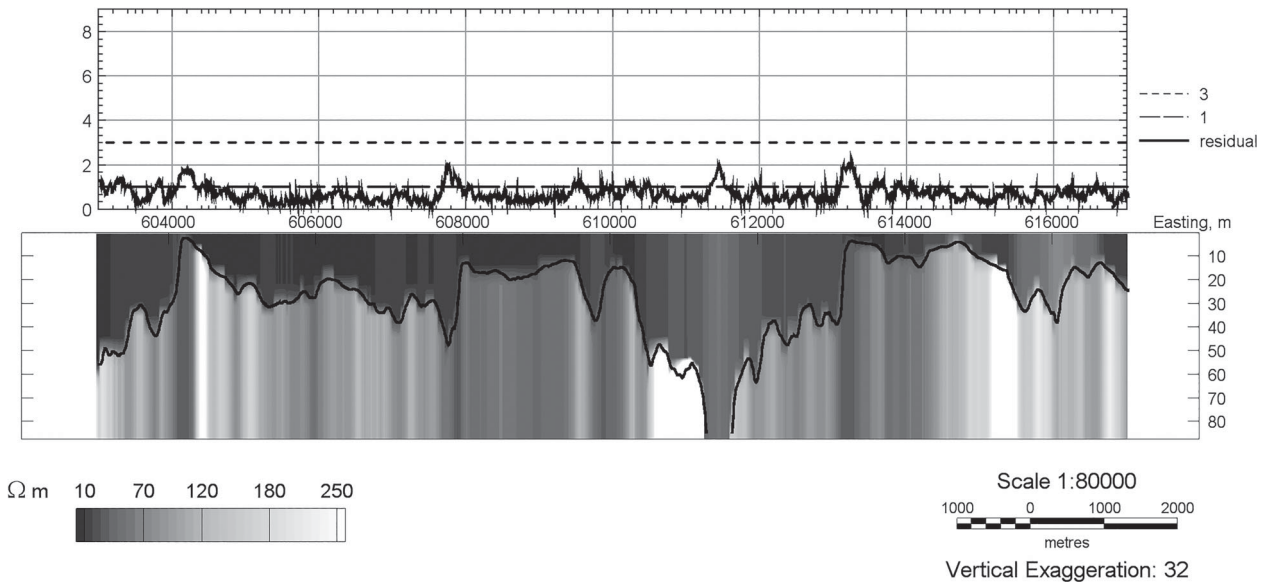


Figure 5. LCI-like 1D inversion for the two-layered model (lower) and residuals (upper).

two-layered model allows the noises to affect the solution; and so gives us a reason to apply smoothing.

To obtain an LCI-like solution I use a prognosis step (Equation 9) of IEKF with trivial deterministic part ($\mathbf{f}(\mathbf{x}) = \mathbf{x}$). Matrix \mathbf{Q} has a diagonal form: $\text{diag}\{0.005, 0.005, 0.005\}$. This means that each parameter from one point to another changes by $\sim 0.5\%$. The result is shown in Figure 5. Here, we get a less-noisy solution having almost the same residuals.

Conclusions

The inversion problem for AEM is an essential part of data processing. A variety of methods is available, even for a 1D case. Sometimes choice of the most appropriate method may be quite sophisticated. The method described in this article considers AEM data inversion as a stochastic estimation problem and uses well-developed tools of estimation theory based on the Kalman filter. As a result, it allows combination of the modern approaches to inversion and provides an efficient solution for various types of environment. The results of the algorithm application are shown using several examples – the apparent resistivity calculation and 1D inversion for FD AEM system EM4H.

The algorithm automatically estimates the influence of each component of the measurement vector. It provides a smooth and unique solution for conditions where traditional methods have difficulties. In addition, the method takes into account the geometry of the system. It allows flight restrictions to be avoided: substantial variations in flight speed or even variations in flight altitude in a certain diapason do not lead to substantial distortions in the obtained apparent resistivity.

It is worth noting that the described algorithm converges rapidly. In the considered examples, the solution was achieved in one or two iterations in each case.

References

- Chang-Chun, Y., R. Xiu-Yan, L. Yun-He, Q. Yan-Fu, Q. Chang-Kai, and C. Jing. 2015. Review on airborne electromagnetic inverse theory and applications. *Geophysics* 80, no. 4: W17–31.
- Fraser, D.C. 1987. Layered-earth resistivity mapping. In *Developments and applications of modern airborne electromagnetic surveys*, ed. D.V. Fitterman, 33–41. Golden, Colo., USA: US Geological Survey Bulletin.
- Golovan, A.A., and N.A. Parusnikov. 1998. A relationship between the stochastic estimability measure and singular matrix expansions. *Automation and Remote Control* 59, no. 2: 190–93.
- Guillemoteau, J., P. Sailhac, and M. Béhaegel. 2011. Regularization strategy for the layered inversion of airborne transient electromagnetic data: Application to in-loop data acquired over the basin of Franceville (Gabon). *Geophysical Prospecting* 59: 1132–43.
- Hadamard, J. 1932. *Le problème de Cauchy et les équations aux dérivées partielles linéaires hyperboliques*. Paris, France: Hermann.
- Havlik, J., and O. Straka. 2015. Performance evaluation of iterated extended Kalman filter with variable step-length. *Journal of Physics: Conference Series* 659: 12–22.
- Jupp, D.L.B., and K. Vozoff. 1975. Stable iterative methods for the inversion of geophysical data. *Geophysical Journal of the Royal Astronomical Society* 42: 957–76.
- Kalman, R. 1960. A new approach to linear filtering and prediction problems. *ASME Journal of Basic Engineering* 82: 35–45.
- Karshakov, E., and J. Moilanen. 2018. Combined interpretation both time domain and frequency domain data. Papers of the 7th International Workshop on Airborne Electromagnetics AEM-2018, 1–3. Kolding, Denmark.
- Karshakov, E.V., and M.V. Kharichkin. 2008. A stochastic estimation problem at aeromagnetometer deviation compensation.

- Automation and Remote Control* 69, no. 7: 1162–70.
- Keppenne, C.L., and M. Rienecker. 2003. Assimilation of temperature into an isopycnal ocean general circulation model using a parallel Ensemble Kalman filter. *Journal of Marine Systems* 40–41: 363–80.
- Legault, J.M. 2015. Airborne electromagnetic systems – State of the art and future directions. *CSEG Recorder* 40 no. 6: 38–49.
- Palacky, G.J. 1987. Resistivity characteristics of geologic targets. In *Electromagnetic Methods in Applied Geophysics - Theory*, ed. N. M. Nabighian, 53–129. Tulsa, Oklahoma, USA: Society of Exploration Geophysics.
- Simon, D. 2006. *Optimal state estimation. Kalman, H_∞ and nonlinear approaches*. Hoboken, NJ: John Wiley & Sons, Inc.
- Volkovitsky, A., and E. Karshakov. 2013. Airborne EM systems variety: what is the difference? Mpumalanga, South Africa. Papers of the 13th SAGA Biennial @ 6th International AEM Conference AEM-2013, 1–4.
- Vovenko, T., E. Moilanen, A. Volkovitsky and E. Karshakov. 2013. New abilities of quadrature EM systems: Mpumalanga, South Africa. Papers of the 13th SAGA Biennial @ 6th International AEM Conference AEM-2013, 1–4.
- Zhdanov, M.S. 2009. *Geophysical electromagnetic theory and methods*. Amsterdam, Netherlands and Oxford, UK: Elsevier.